Journal of Materials Engineering and Performance
ASM INTERNATIONAL

The Correlation between the Percussive Sound and the Residual Stress / Strain Distributions in a Cymbal

Journal:	*Journal of Materials Engineering and Performance*
Manuscript ID	JMEP-16-08-11209.R2
Manuscript Type:	Technical Paper
Date Submitted by the Author:	28-Sep-2016
Complete List of Authors:	Osamura, Kozo; Research Institute for Applied Sciences, Kuratani, Fumiyasu; Fukui University, Department of Mechanical Engineering Koide, Toshio; Koide Cymbals Ogawa, Wataru; Osaka Alloying Works Taniguchi, Hiroyasa; Osaka Alloying Works Monjyu, Yoshiyuki; Osaka Alloying Works Mizuta, Taiji; Osaka Alloying Works Shoubu, Takahisa; Japan Atomic Energy Agency, Quantum Beam Science Center
Keywords:	cymbal, tin-copper alloy, residual strain, synchrotron radiation

The Correlation between the Percussive Sound and the Residual Stress / Strain Distributions in a Cymbal

Kozo Osamura[a)], Fumiyasu Kuratani[b)], Toshio Koide[c)], Wataru Ogawa[d)], Hiroyasu Taniguchi[d)], Yoshiyuki Monju[d)], Taiji Mizuta[d)], and Takahisa Shoubu[e)]

a) Research Institute for Applied Sciences, Sakyo-ku, Kyoto, 606-8202, Japan
b) Department of Mechanical Engineering, University of Fukui, 3-9-1 Bunkyo, Fukui, 910-8507, Japan
c) Koide Works, Ltd. (Koide Cymbals), 1-22-32 Kamisyoukakuji, Hirano-ku, Osaka, 547-0006, Japan
d) Osaka Alloying Works, Co., Ltd., 45-5-9 Shirakata, Fukui, 910-3138, Japan
e) Japan Atomic Energy Agency, Sector of Nuclear Science Research Quantum Beam Science Center, 1-1-1 Kouto, Sayo-cho, Sayo-gun, Hyogo 679-5148, Japan

Abstract

The artistic sound of a cymbal is produced by employing a special copper alloy as well as incorporating complicated and heterogeneous residual stress / strain distributions. In order to establish a modern engineering process that achieves high quality control for the cymbals, it is necessary to investigate the distribution of the residual stresses / strains in the cymbal and their quantitative relation with the frequency characteristics of the sound generated from the cymbal. In the present study, we have successfully used synchrotron radiation to measure the distribution of residual strain in two kinds of cymbals - after spinforming as well as after hammering. The microstructure and the mechanical properties of the cymbals were measured as well their acoustic response. Based on our experimental data, the inhomogeneous residual stress / strain distributions in the cymbals were deduced in detail and their influence on the frequency characteristics of the sound produced by the cymbals were identified.

Keywords: cymbal, tin – copper alloy, residual strain, synchrotron radiation, artistic sound

1. Introduction

The cymbal is a percussion instrument that has existed since ancient times and was made from bell metal [1]. It is normally fabricated using one part tin to four parts copper, that is 20% tin. But there have always been some variations. Depending on the manufacturer, some small but significant amounts of other elements, notably silver, gold, phosphorus and so on, are added. Bell bronze is a two-phase alloy that includes a major beta phase and a minor alpha phase. These two phases make the metal harder and more brittle than a single-phase alloy, affect the hardening process (produced by hammering and lathing), and greatly restricting the use of mechanized techniques for manufacture.

A typical and traditional process for fabricating a cymbal is shown in Table 1. Cymbals are made from individually cast ingots which are then hot-forged to form the rough shape of the cymbal. The forming process then consists of cupping and spinforming using a spatula to deform the metal into a domed shape in order to introduce a graded residual stress. In the next turning process, hammering is added to unevenly harden the metal and then the thickness is reduced using a lathe. Particularly the spinforming and hammering must be entirely performed by a highly skilled hand and both labour-intensive processes. These complicated processes that generate the inhomogeneous residual strain produce much of the unique and characteristic musical sound of the cymbal. This effect is often deliberately enhanced by use of a coarse lathe tool, and sometimes by a very limited final polishing, leaving the lathe tool marks as tone grooves. The broad process for fabricating cymbals mentioned here, is modified by individual manufacturers. It is important to understand how these modifications result in more consistent sounding cymbals.

Table 1 Process for fabricating a cymbal

Process	Detailed Operation
Original Plating	Ingot Casting
	Hot Forging
Forming	Cupping
	Spinforming
	Thickness Adjusting
Turning	Hammering
	Lathing
Finishing	Thickness Adjusting
	Polishing

As emphasized above, the fabrication of a cymbal has been developed by experts during a long process of using both traditional and empirical techniques. In general, the sound produced by cymbals has three characteristics: a loud sound, a complicated tone and a long echo. They are all very sensitive to the forming and turning processes. If we can puzzle out a numerical description of each step of these fabrication processes, it becomes possible to establish a modern engineering process for achieving high quality control as well as creating the possibility for completely new-sounding cymbals. As a first step to establishing such an engineering fabrication methodology, it is important to make clear the distribution of inhomogeneous residual stress / strain in the cymbal and its relation with the frequency characteristics of generated sound from the cymbal.

Cymbals vibrate in many different mode shapes and radiate sounds with complex overtones. Their characteristic behaviour has been investigated by means of the measurement of vibration modes [2, 3] and the numerical analysis of mode coupling and nonlinear vibrations [4, 5]. The sound of a cymbal depends on its size and shape and also the manufacturing process (cf Table 1). Even though the sound produced is very sensitive to processing, very few studies have been done on the effect of the manufacturing process until now.

In the present study, two kinds of cymbals (after spinforming as well as after hammering) were investigated using a beam of synchrotron radiation to determine the distribution of residual strain. Also microstructural and mechanical properties were measured as well as acoustic properties. On the basis of our experimental data, the inhomogeneous residual strain distribution in the cymbals was deduced in detail and their influence on the frequency characteristics of the sound discussed.

2. Experimental Procedure

2.1 Samples

Two kinds of cymbals, prepared by KOIDE Cymbal, were used in our present study. The alloy used for the cymbals was Cu-23%Sn-0.3%Ti alloy [6], which was fabricated by Osaka Alloying Works. As mentioned in the previous section, one of them was the cymbal after spinforming and the other was produced first by spinforming and then hammered as shown in Fig. 1. After the spinning process, the cymbal has a domed shape with diameter of 406 mm and thickness of 2 to 4 mm.

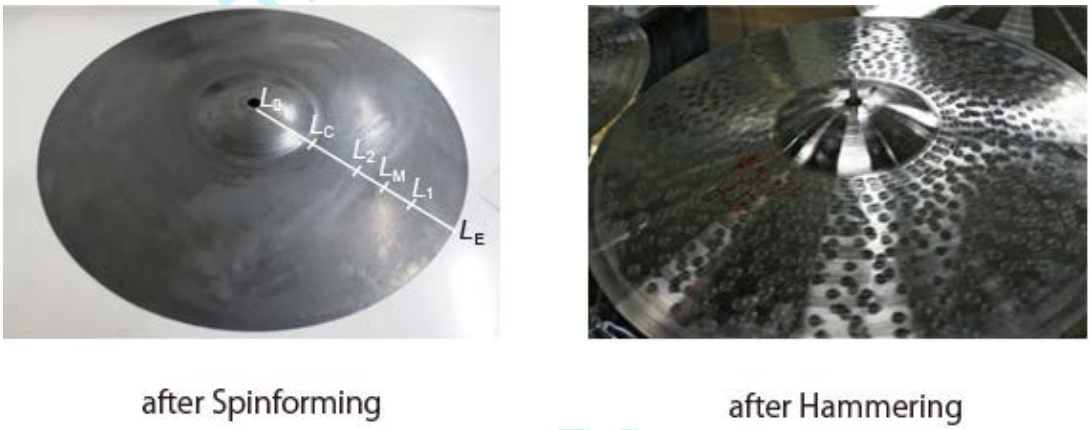

Fig. 1 The top surface of the two cymbals tested (LHS) after spinforming and (RHS) after hammering.

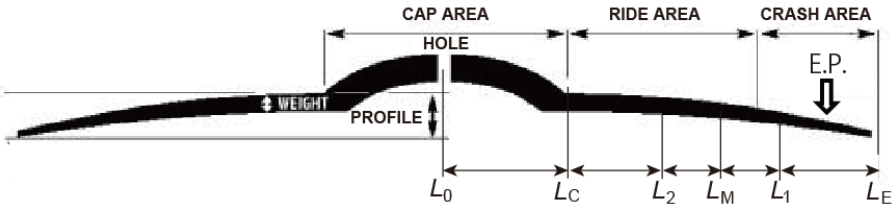

Fig. 2 The areas analyzed for residual strain distribution, where E.P. indicates the excitation point for the acoustic measurements.

2.2 Residual strain measurements

The diffraction experiments were carried out at room temperature at the BL28B2 station of SPring-8. It used white X-rays with energies between 30 and 150 keV with two cooled Ge solid-state detectors set to a diffraction angle of $2\theta = 11^{o}$ at the vertical direction (dv) and horizontal one (dh). The cymbal (s) was placed on the goniometer as

shown in Fig. 3. Here the data accumulated using the vertical detector (dv) are reported, which give information about the strain along the circumferential direction. The slit sizes used were 0.05x0.05 mm^2 for the entrance and 0.05x5.0 mm^2 for the exit. In addition, a collimator with cross-sectional area 0.05x5 mm^2 and 150 mm length was placed behind the exit slit in order to restrict the gauge volume.

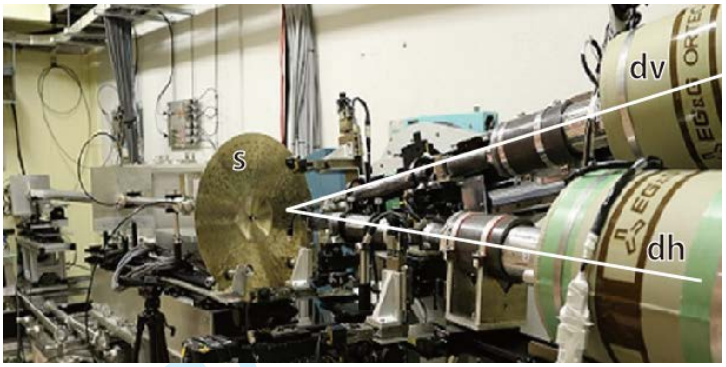

Fig. 3 Layout of the cymbal (s) and detectors (dv and dh) for measuring the residual strain in the cymbal. The bottom surface of the cymbal is clearly shown.

The points selected for analysis were chosen as follows: As shown in Figs. 1 and 2, the center of the area chosen for analysis was at L_1 where the radius of (L_1-L_0) was about 160 mm and the radius of cymbal (L_E-L_0) was 203 mm. In order to investigate the distribution of local residual strain at L_1, the cymbal was shifted along the horizontal direction (x–direction) step by step as shown in Fig. 4, where the central coordinate x_0 of the hammering depression was set at the center of hammering depression close to L_1. Each shift along x-direction for each step was x_i-x_{i-1} = 1 mm. At each step, the cymbal was also shifted in the depth direction (y-direction) so the beam was focused at positions from the top surface of the cymbal (cf Fig. 1) to the bottom surface. By these means, a total of 49 different diffraction data sets were accumulated from locations throughout the volume of each cymbal. In the case of the cymbal after spinforming, where the surface of the cymbal was relatively smooth, the measurements were carried out in the same area (i.e. at L_1) as shown in Fig. 1.

Because a white X-ray source was employed, multiple diffraction peaks were observed. In the present experimental conditions, they were the (110), (220), (222), (400) and (420) peaks of the β-phase and the (311), (331), (420), (551) and (533) peaks of the α-phase. An example of part of the experimental procedure is provided by considering the data shown in Fig. 5: The (222) diffraction peak for the β-phase was detected while shifting each analyzing position from y= -0.8 mm to 1.2 mm. Figure

5 shows that the lattice spacing increases as the analysis position changes from the bottom surface to the top one. In the present study, the spacing of the (420) plane was employed for residual strain measurements because the (420) diffractions were observed most frequently and its diffraction intensity was strong enough to ensure sufficient statistical accuracy. The strain (A) was calculated from the observed lattice constant (a) of the β-phase by using the relation $A = (a - a_0)/a_0 \cdot 100$ [%], where a_0 is the data for an unstrained powdered sample.

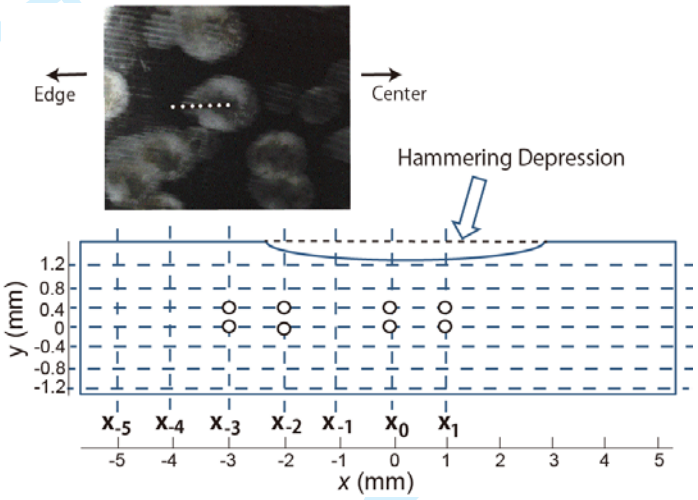

Fig. 4 Analyzing positions at and around a hammering depression

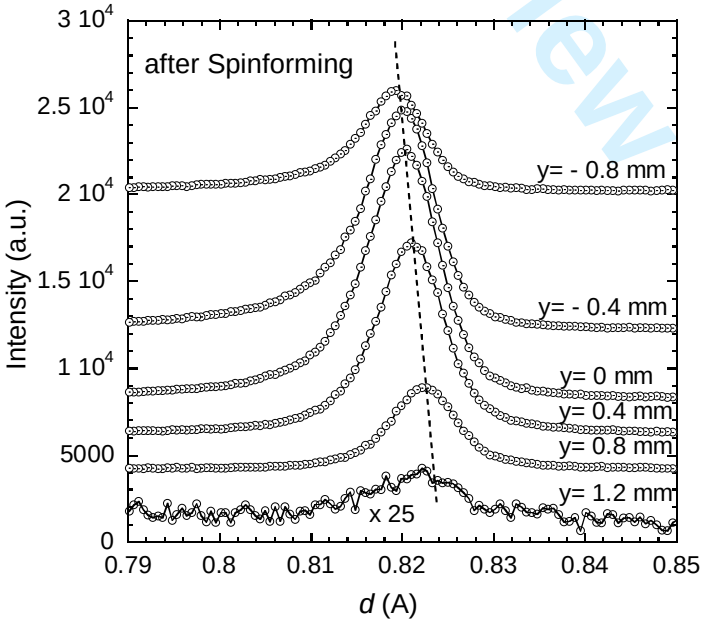

Fig. 5 The (222) diffraction peak for the β -phase obtained by analyzing positions from y= -0.8 mm to 1.2 mm in the cymbal after spinforming

2.3 Microstructure analysis and tensile test

After the residual strain measurements, the cymbals were cut for the microstructural analysis as well as tensile testing. The microstructural analysis was carried out using an electron probe micro-analyzer (EPMA JEOL JXA-8500F). Tensile testing was carried out at room temperature using a tensile machine Shimadzu AG-50kNIS. The initial distance between chucks was kept as 100 mm. A Nyilas type double extensometer (GL = 25 mm) was attached at the center of the sample. The initial cross head speed was selected as $1.67 \times 10^{-5}[s^{-1}]$.

2.4 Acoustic Measurement

In order to investigate the change of sound due to the forming and turning processes, acoustic measurements were performed. In general, the sound spectrum changes depending on the position of the excitation point and the position for accumulating the sound data. The main purpose of our study was to investigate the influence of the different fabrication stages on the sound spectra. So, we kept the conditions for the acoustic measurements on both cymbals the same: The cymbal was struck using the impulse hammer with 40 N at the excitation point (E.P.) shown in Fig. 2, which was located at about 20 mm from the edge. The sound radiation was measured using a microphone placed 100 mm away from the edge of cymbal. The sampling time and frequency were 2.56 s and 25600 Hz, respectively. Eventually 65,536 data were Fourier – transformed to provide the frequency spectra.

3. Experimental Results

3.1 Microstructure

Fig. 6 shows the microstructure of the cymbal after the hammering. It is heavily deformed with a coarse grained polycrystalline microstructure. The matrix and the precipitates were analyzed using EPMA and found to be β^- and α -phases respectively. The microstructural observations showed that no micro-cracks occurred in the cymbal after the hammering. On the other hand, the general experience with cymbals is that most of them are eventually damaged by cracks after extensive use. The main reason for the cracking is predominantly related to the plastic deformation at

and around the region where the cymbal stick strikes the cymbal during use. It is known, that one factor that determines the lifetime of the cymbal relates to its deformability, the so-called 'softness' of the cymbal itself, but it is not yet clear how this relates to the depressed areas produced by hammering.

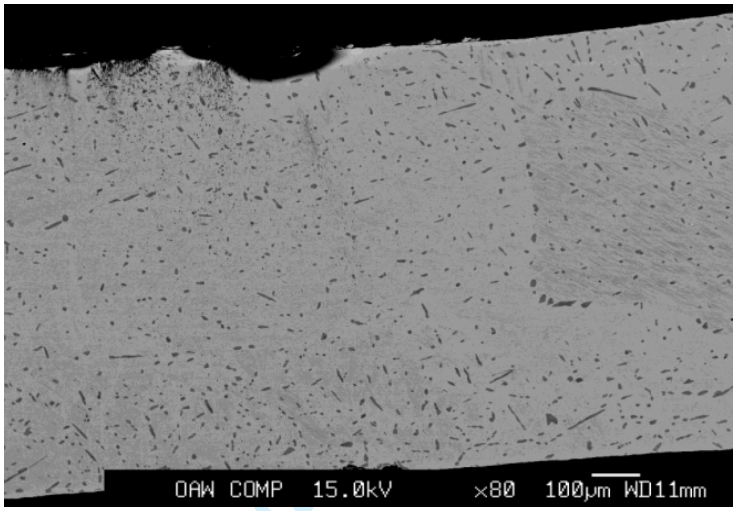

Fig. 6 Cross section of the cymbal after the hammering

3.2 Tensile Properties

Fig. 7 shows the stress – strain curves for the two samples quarried along the circumfrential direction of cymbals after spinforming and hammering. Their tensile properties were almost the same, - the Young's modulus (E) and the 0.2% proof stress ($R_{0.2}$) were determined as 80.8 GPa and 384 MPa, respectively.

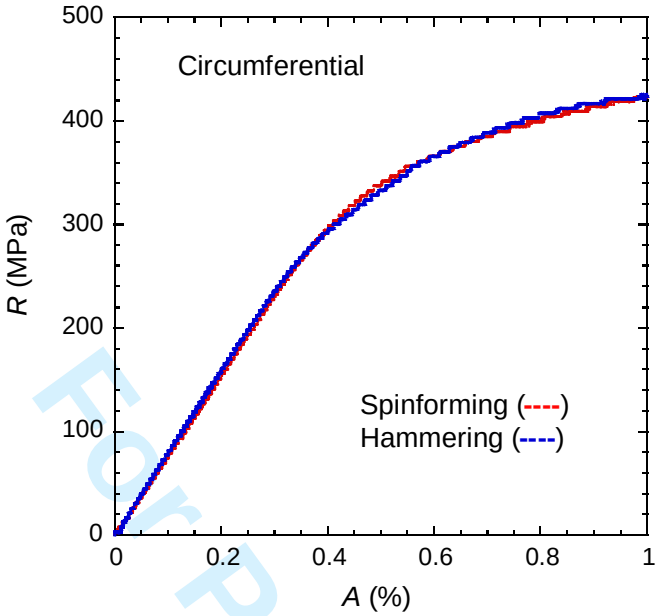

Fig.7 Stress vs strain curve for the two samples quarried from the cymbals after spinforming and hammering.

In order to evaluate the stress corresponding to the local strain, it is necessary to establish the functional relationship between stress and strain. For this purpose, the following equation was applied [7],

$$R = \frac{Eb(A)^{1+1/n}}{EA + b(A)^{1/n}} \qquad (1)$$

Where E, b and n are the fitting parameters. The result of curve-fitting is shown in Fig. 8, where the open circles are the calculated results using Eq.(1). The calculated results were found to fit the experimental data well, where E=80.8 GPa, b=900 and $1/n$ = -1.1.

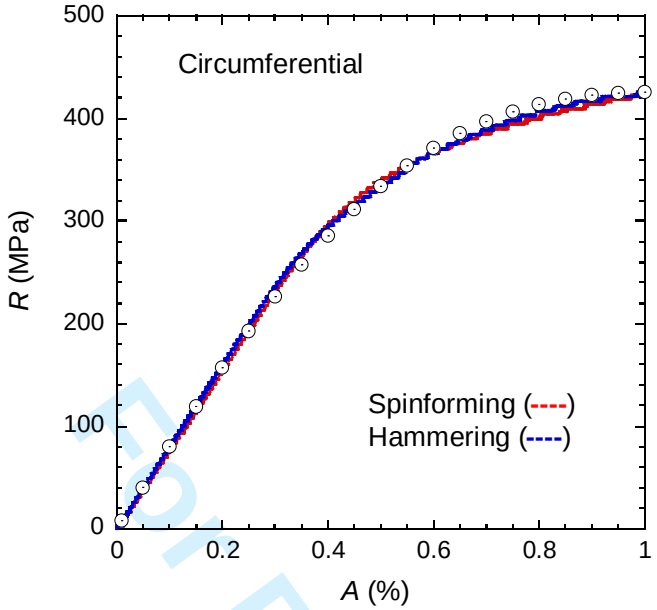

Fig.8 Result of the curve-fitting of Eq. (1) to the experimental data, where the open circles are the calculated results

3.3 Residual strain measurement

For each cymbal, diffraction data were measured at 49 coordinates of (x_i, y_i) as shown in Fig. 4. At each position, different combinations of diffraction peaks were observed because in these coarse grained polycrystalline samples, the crystal orientation of the β-phase grains from which most scattering occurred, changed from position to position. Although the lattice constant derived from all equivalent diffraction peaks is the same, in practice it is not possible to determine an *absolute value* of the lattice constant to within an accuracy of higher than 0.02 %. As such, in the present paper, we have determined the *relative change* of lattice parameter from the strong (420) diffraction peak of the β-phase in our analysis. This ensures the precision is better than 0.015 %.

Fig. 9(a) shows the change of lattice parameter of the β-phase from the bottom surface to the center of the thickness of the cymbal after spinforming, around the position L_1. The experimental data are given in the range of between y = -1.2 and 0 mm. None of the β (420) diffraction peaks were observed in the remaining range between y = 0.4 and 1.2 mm. As shown in Fig. 9(a), the lattice parameter increased linearly from the bottom surface to the top. The lattice parameter changes that were observed in the thickness direction were similar for all the x_i positions from x_1 to x_{-2}. The residual strain became zero at the center of cymbal (y = 0 in Fig. 9(a)). The average lattice parameter for four experimental data at y = 0 was evaluated to be $a_0(\beta)$=2.8315 A. Thus, given

the linearity and the repeatability observed, we can assume that for the spinforming cymbal, the lattice parameter at the top surface can be found by extrapolating, using the dotted line shown in Fig. 9(a). On the other hand, the magnitude of the lattice parameter and the changes in lattice parameter were different for the different x_i positions for the cymbal after hammering as shown in Fig. 9(b). Nevetheless, we found that the lattice parameter broadly increased linearly with increasing y position again (i.e. from the bottom surface to the top).

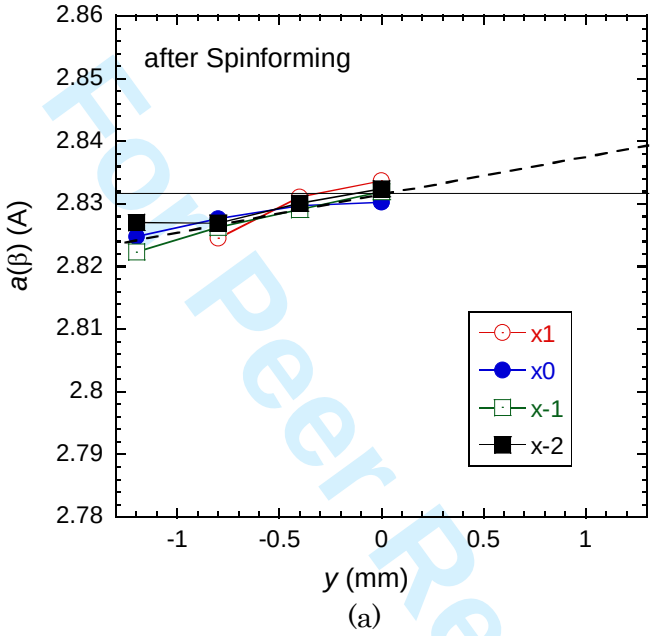

(a)

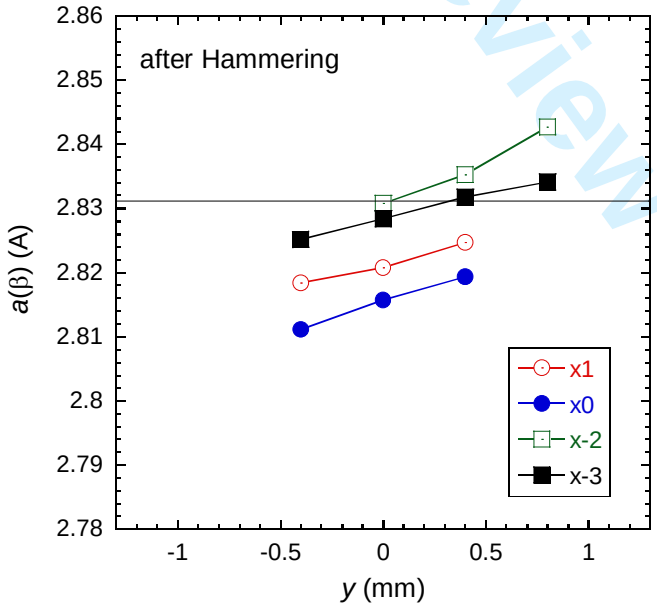

(b)

Fig. 9 Change of the lattice parameter of β-phase as a function of the depth coordinate y for the cymbals after the spinforming (a) and the hammering (b).

3.4 Residual strain distrribution

Using the lattice parameter data shown in Fig. 9, the residual strain was evaluated. The change of residual strain along the thickness direction is shown in Fig. 10 for the cymbal after spinforming. The maximum compressive strain at the bottom surface (y= -1.2mm) was on average of -0.24 %. The compressive strain reduced linearly towards the center. The strain distributions were nearly the same, independent of the x_i positions. Hence using extrapolation, we found that the maximum tensile strain at the top surface was estimated to be 0.24 % at y = 1.2mm.

The change of residual strain as a function of thickness is shown in Fig. 11 for the cymbal after hammering. The magnitude of residual strain was quite strongly dependent on the x_i position. Here (to aid with comparison) the dotted line indicates the distribution of residual strain in the cymbal after spinforming. The residual strains tend to shift towards the compressive strain side at the centre of the hammered depression (i.e. at x_0) as expected, while the residual strain increased with increasing y position from the bottom surface to the top surface. Within the experimental data indicated here, the maximum compressive strain was recorded as 0.71 % at y= -0.4 mm of x_0.

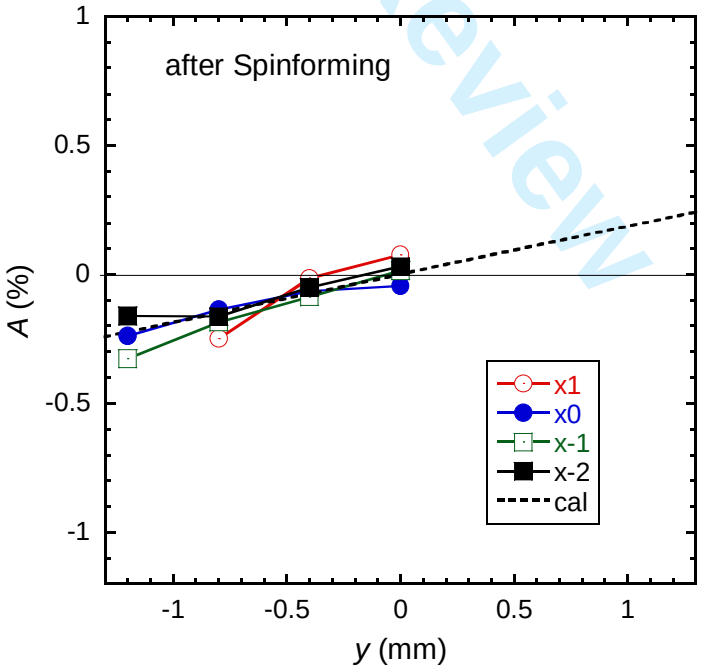

Fig. 10 Residual strain distribution as a function of thickness for several x_i positions for the cymbal after spinforming

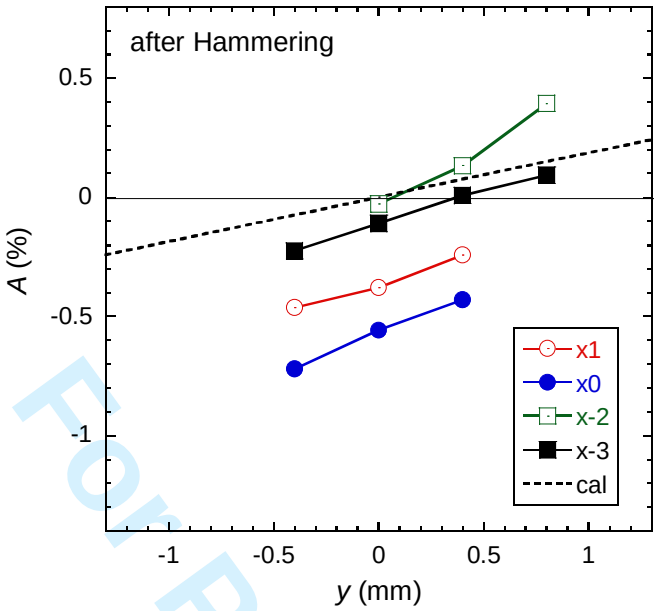

Fig. 11 Residual strain distribution as a function of thickness for several x_i positions for the cymbal after hammering.

3.3 Residual stress distribution

The residual stress was evaluated from the residual strain by using the functional relation given by Eq. (1). The residual stress distribution as a function of thickness is shown in Fig. 12 for the cymbal after spinforming. The maximum compressive stress generated at the bottom surface (at y= -1.2 mm) had an average of -172 MPa. When extrapolating to the top surface (at y = 1.2 mm), the maximum tensile stress was found to be 172 MPa.

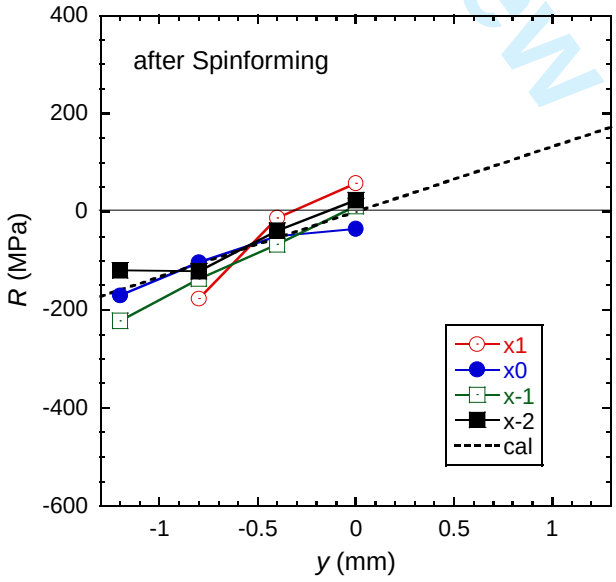

Fig. 12 Residual stress distribution as a function of thickness for several x_i positions for the cymbal after spinforming

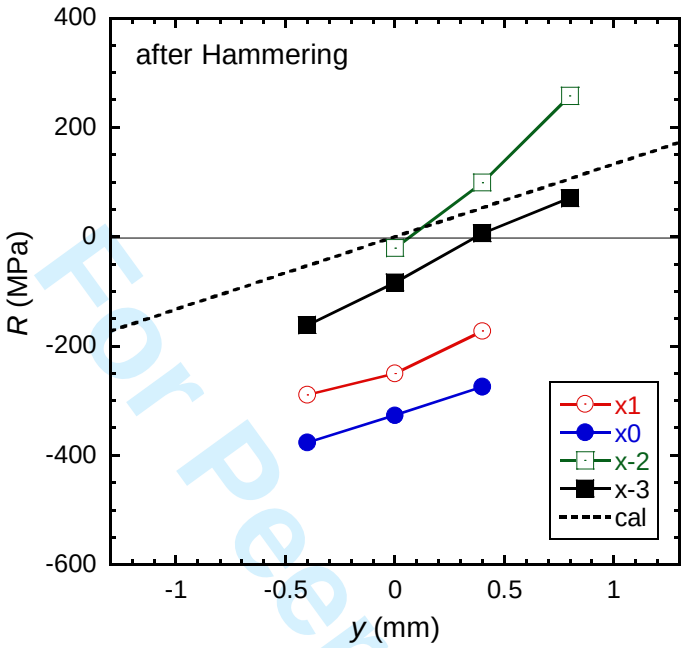

Fig. 13 Residual stress distribution as a function of thickness for several x_i positions for the cymbal after hammering.

The change of residual stress for the cymbal after hammering is shown as a function of thickness in Fig. 13, where the dotted line indicates the distributuion of residual stress in the cymbal after spinforming. The stress was mostly compressive. The maximum compressive stress measured was -376MPa and the maximum tensile stress was 257MPa as far as the experimental data are shown in Fig. 13.

3.4 Strain / stress distribution around a hammaring depression

The depressions (as shown in Fig. 4.) were produced by hammering. The strain and stress distribution around a depression are shown in Figs. 11 and 13. Instead of Fig. 11, where the residual strain around a hammering depression is plotted as a function of y, four experimental data points at y = 0 and 0.4 mm are plotted as a function of $(x_i - x_0)$ and shown in Fig. 14. If it is assumed that the distributuion of residual strain is symmetric around the depression, it is possible to link each four experimental data and to depict the distribution as shown by the dotted lines. Thus we can see the broad features of the residual strain distribution around the hammering depression. At the

centre of the depression, the residual strain is strongly compressive but at the outer circumference of the depression, the residual strain can become tensile. The residual strains are more strongly compressive as one approaches the back of the cymbal (comparing y = 0.4 mm with that at y = 0 mm). Using the same procedure, the distribution of residual stress around a hammering depression was estimated as shown in Fig. 15. The maximum compressive stress was 330 and 273 MPa at y = 0 and 0.4 mm, respectively.

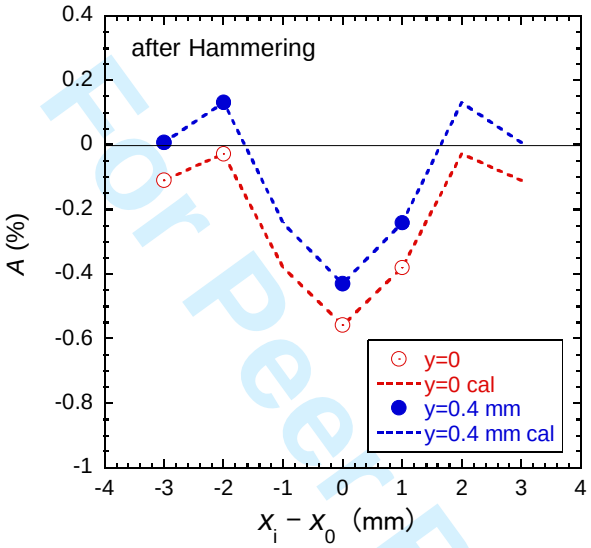

Fig. 14 Estimated distribution of residual strain around a hammering depression for the cymbal after hammering

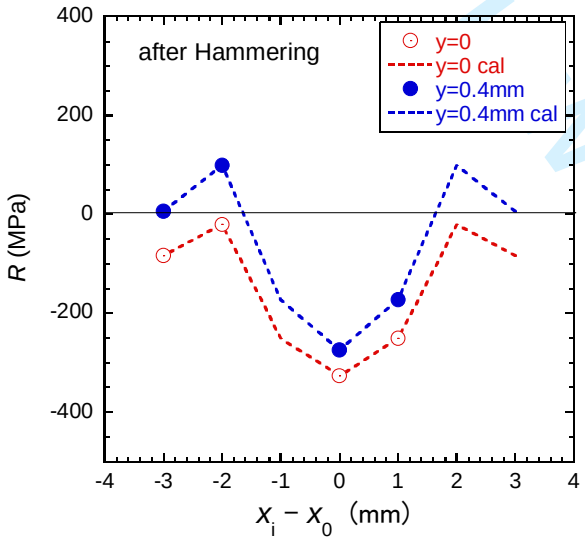

Fig. 15 Estimated distribution of residual stress around a hammering depression for the cymbal after hammering

3.5 Frequency distribution of sounds

Typical results from our acoustic measurements, in the frequency range of human audible sound, are shown in Fig. 16. The frequency dependence of the sound pressure is indicated in the range between 0 and 8 kHz for both cymbals (i.e. after spinforming and after hammering). Several pressure peaks are observed. A common feature for both cymbals was the eight large peaks indicated by ▽. Their intensities are stronger by 29 % on average for the hammered cymbal. The second feature was that the peak indicated by ▲ that appears for the cymbal after spinforming, but disappers after hammering. The third feature was that several new peaks indicated by ▼ appear for the cymbal after hammering. In general, the peak intensities (sound pressure) are stronger for the hammered cymbal. So it is clear that the hammering offers a pronounced effect, generating intense and complicated artistic sounds.

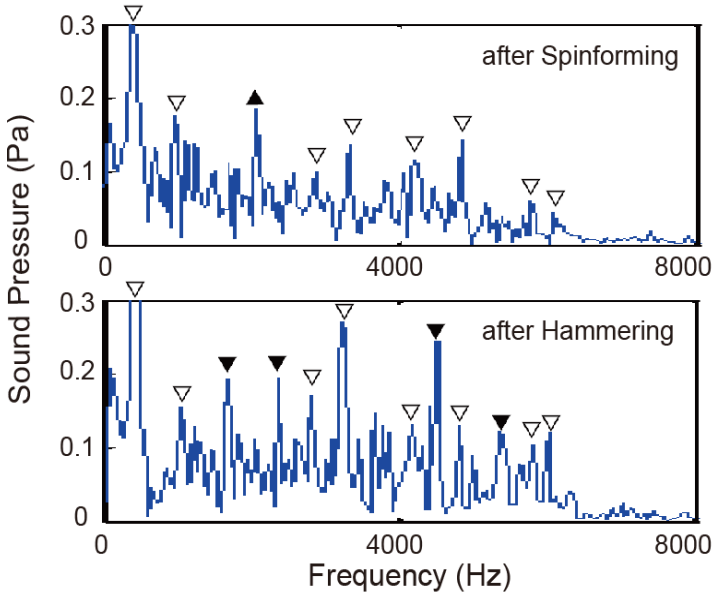

Fig. 16 Frequency dependence of sound pressure for two cymbals after spinforming and after hammering

4. Discussion

Empirically it has been long recognized that the spinforming provides the basic frequency pattern of the cymbal which consists of the wide distribution from low to high frequencies. The hammering increases the intensity of the sound from the cymbal (cf Fig. 16) and strongly modifies the frequency distribution particularly enhancing the high frequency components. The successive lathing and finishing processes modifies

the sound pressures produced.

Thus the special sounds produced by the cymbals should be strongly related with the storaged large residual stress / strain in the cymbal. The deformation into the cup shape during the spinforming process produced stored compressive and tensile stress / strain which were found to have maximum amplitudes of 344 MPa / 0.34%, respectively. The additional inhomogeneous deformation produced during the hammering process produced very large additional stored compressive stresses / strains reaching to 376 MPa / 0.71 % at the center of hammering depression.

This work shows that the latter inhomogeneous stress / strain distribution at the hammering depression strongly affects the frequency distribution. It has also been recently analyzed by one of coauthors using finite element analysis (FEA) [4, 8] and also by applying a thermal stress to reproduce a local stress distribution. The FEA/thermal results showed each mode of the cymbal has a different sensitivity to the thermal load. The eigenfrequencies of some modes decreased as the bending modulus decreased. This led to a change in the frequency response and in the deformation shape by hammering that significantly improved the sound radiation efficiency. The experimental observations of the change in frequency distribution mentioned in Section 3.5 are qualitatively consistent with the results from the FEA.

A similar technique of storing residual stress/strain has been used to improve circular saws for cutting wood [9]. This approach suppresses "snaking" in the circular saw when it rotates at or close to its critical speed. This is a vibrational resonance phenomenon called critical speed instability [10]. In order to reduce this instability, the saws can be “tensioned” to increase the dynamic stiffness of saws. Typically, the tensioning is carried out by hammering or rolling the sawblade surfaces. Further new techniques such as heat tensioning and thermal tensioning are also becoming popular. In all of these methods, the tensioning induces stored in-plane stresses in the sawblade. When favorably distributed, these stresses substantially stiffen the sawblade and improve its cutting stability. However according to Barz [11], hammer tensioning is very much an art, and great skill and experience is required to achieve good results. When done well, hammering can be as effective as more modern methods. However, hammer tensioning is usually not recommended for general use because the results can be very variable. Also, the hammer blows make the sawblade surface uneven and can initiate fatigue cracks. It is emphasized that the various techniques using for “tensioning” circular saws might yet offer routes for further improvement of cymbals

5. Summary

The artistic sounds of a cymbal are realized by employing a special copper alloy as well as the creation of complicated and inhomogeneous residual stress / strain distributions by an expert in the art. In order to establish modern engineering processes to achieve high quality control of cymbals, it is necessary to investigate the distribution of residual stress / strain in the cymbal and their quantitative relation with the frequency characteristics of the sound generated by the cymbal.

In the present study, we have succeeded in measuring the distribution of residual strain in two kinds of cymbals after spinforming as well as after hammering, by means of synchrotron radiation. We have also measured their microstructure, mechanical properties and acoustic response. On the basis of these experimental data, the inhomogeneous residual stress / strain distribution in the cymbals was measured and analyzed in detail and their influence on the frequency characteristics of the sound was identified and discussed.

Acknowledgements:
The authors express their hearty thanks for Dr Kentaro Kajiwara of JASRI for his valuable scientific suggestion and experimental support. The diffraction experiments were performed at BL28B2 of Spring-8 as the research subject of industrial application (Proposal No. 2013A1346).

References

[1] N. H. Fletcher and T. D. Rossing; The Physics of Musical Instruments, Springer - Verlag (1998)
[2] G. D. Giulio, E. Esposito, C. Santolini and L. Scalise; Experimental Vibrational Analysis of Drum Cymbals, Proceedings of the 19th International Modal Analysis Conference, 2001, 724-730
[3] R. Perrin, G. M. Swallowe, S. A. Zietlow, and T. R. Moore; The normal modes of cymbals, Proceedings of Spring Conference of the Institute of Acoustics 2008: Widening Horizons in Acoustics, Proceedings of the Institute of Acoustics Vol. 30. Pt.2, pp.460-467, 2008
[4] T. Kawai, F. Kuratani, T. Yoshida and T. Masumoto; Sound Radiation Characteristics of Cymbals based on Mode Shapes, Proceedings of 52th JSME Hokuriku Shin-etsu branch conference, Paper No.0311, (2015) (in Japanese).
[5] A. Chaigne, C. Touze´ and O. Thomas; Nonlinear vibrations and chaos in gongs and cymbals, Acoust. Sci. & Tech. 26, 5 (2005) pp.403-409
[6] http://koidecymbal.com/lineup/index.html

[7] K. Osamura, S. Machiya , Y. Tsuchiya , H. Suzuki, T Shobu, M Sato, S. Harjo, K. Miyashita, Y. Wadayama, S. Ochiai and A. Nishimura; Thermal Strain Exerted on Superconductive Filaments in Practical Nb_3Sn and Nb_3Al Strands, Supercond. Sci. Technol. 26 (2013) 094001 (8pp).

[8] F Kuratani, T Yoshida, T Koide, T Mizuta and K Osamura, Understanding the effect of hammering process on vibration characteristics of cymbals, MoViC RASD (2016)

[9] G.S. Schajer; Understanding saw tensioning, Holz als Rob- und Werkstoff 42 (1984) 425~430

[10] C. D. Mote Jr and L. T. Nieh; On the foundation of circular-saw stability theory. Wood and Fiber 5 (1973) 160-169

[11] E. Barz,: Vergleichende Untersuchungen ueber das Spannen von Kreissaegeblaettern mit Maschinen und mit Richthaemmern. (Comparative studies of tensioning of circular sawblades with machines and by hammering). Holz Rob und Werkstoff 21 (1963) 135-144. CSIRO Australia Translation No. 6583